Direct Measurement of the W Boson Width in $p\bar{p}$ Collisions at $\sqrt{s} = 1.96$ TeV

T. Aaltonen,[23] J. Adelman,[13] T. Akimoto,[54] M. G. Albrow,[17] B. Álvarez González,[11] S. Amerio,[42] D. Amidei,[34] A. Anastassov,[51] A. Annovi,[19] J. Antos,[14] M. Aoki,[24] G. Apollinari,[17] A. Apresyan,[47] T. Arisawa,[56] A. Artikov,[15] W. Ashmanskas,[17] A. Attal,[3] A. Aurisano,[52] F. Azfar,[41] P. Azzi-Bacchetta,[42] P. Azzurri,[45] N. Bacchetta,[42] W. Badgett,[17] A. Barbaro-Galtieri,[28] V. E. Barnes,[47] B. A. Barnett,[25] S. Baroiant,[7] V. Bartsch,[30] G. Bauer,[32] P.-H. Beauchemin,[33] F. Bedeschi,[45] P. Bednar,[14] D. Beecher,[30] S. Behari,[25] G. Bellettini,[45] J. Bellinger,[58] A. Belloni,[22] D. Benjamin,[16] A. Beretvas,[17] J. Beringer,[28] T. Berry,[29] A. Bhatti,[49] M. Binkley,[17] D. Bisello,[42] I. Bizjak,[30] R. E. Blair,[2] C. Blocker,[6] B. Blumenfeld,[25] A. Bocci,[16] A. Bodek,[48] V. Boisvert,[48] G. Bolla,[47] A. Bolshov,[32] D. Bortoletto,[47] J. Boudreau,[46] A. Boveia,[10] B. Brau,[10] A. Bridgeman,[24] L. Brigliadori,[5] C. Bromberg,[35] E. Brubaker,[13] J. Budagov,[15] H. S. Budd,[48] S. Budd,[24] K. Burkett,[17] G. Busetto,[42] P. Bussey,[21] A. Buzatu,[33] K. L. Byrum,[2] S. Cabrera,[16,r] M. Campanelli,[35] M. Campbell,[34] F. Canelli,[17] A. Canepa,[44] D. Carlsmith,[58] R. Carosi,[45] S. Carrillo,[18,l] S. Carron,[33] B. Casal,[11] M. Casarsa,[17] A. Castro,[5] P. Catastini,[45] D. Cauz,[53] M. Cavalli-Sforza,[3] A. Cerri,[28] L. Cerrito,[30,p] S. H. Chang,[27] Y. C. Chen,[1] M. Chertok,[7] G. Chiarelli,[45] G. Chlachidze,[17] F. Chlebana,[17] K. Cho,[27] D. Chokheli,[15] J. P. Chou,[22] G. Choudalakis,[32] S. H. Chuang,[51] K. Chung,[12] W. H. Chung,[58] Y. S. Chung,[48] C. I. Ciobanu,[24] M. A. Ciocci,[45] A. Clark,[20] D. Clark,[6] G. Compostella,[42] M. E. Convery,[17] J. Conway,[7] B. Cooper,[30] K. Copic,[34] M. Cordelli,[19] G. Cortiana,[42] F. Crescioli,[45] C. Cuenca Almenar,[7,q] J. Cuevas,[11,o] R. Culbertson,[17] J. C. Cully,[34] D. Dagenhart,[17] M. Datta,[17] T. Davies,[21] P. de Barbaro,[48] S. De Cecco,[50] A. Deisher,[28] G. De Lentdecker,[48,d] G. De Lorenzo,[3] M. Dell'Orso,[45] L. Demortier,[49] J. Deng,[16] M. Deninno,[5] D. De Pedis,[50] P. F. Derwent,[17] G. P. Di Giovanni,[43] C. Dionisi,[50] B. Di Ruzza,[53] J. R. Dittmann,[4] M. D'Onofrio,[3] S. Donati,[45] P. Dong,[8] J. Donini,[42] T. Dorigo,[42] S. Dube,[51] J. Efron,[38] R. Erbacher,[7] D. Errede,[24] S. Errede,[24] R. Eusebi,[17] H. C. Fang,[28] S. Farrington,[29] W. T. Fedorko,[13] R. G. Feild,[59] M. Feindt,[26] J. P. Fernandez,[31] C. Ferrazza,[45] R. Field,[18] G. Flanagan,[47] R. Forrest,[7] S. Forrester,[7] M. Franklin,[22] J. C. Freeman,[28] I. Furic,[18] M. Gallinaro,[49] J. Galyardt,[12] F. Garberson,[10] J. E. Garcia,[45] A. F. Garfinkel,[47] H. Gerberich,[24] D. Gerdes,[34] S. Giagu,[50] V. Giakoumopolou,[45,a] P. Giannetti,[45] K. Gibson,[46] J. L. Gimmell,[48] C. M. Ginsburg,[17] N. Giokaris,[15,a] M. Giordani,[53] P. Giromini,[19] M. Giunta,[45] V. Glagolev,[15] D. Glenzinski,[17] M. Gold,[36] N. Goldschmidt,[18] A. Golossanov,[17] G. Gomez,[11] G. Gomez-Ceballos,[32] M. Goncharov,[52] O. González,[31] I. Gorelov,[36] A. T. Goshaw,[16] K. Goulianos,[49] A. Gresele,[42] S. Grinstein,[22] C. Grosso-Pilcher,[13] R. C. Group,[17] U. Grundler,[24] J. Guimaraes da Costa,[22] Z. Gunay-Unalan,[35] C. Haber,[28] K. Hahn,[32] S. R. Hahn,[17] E. Halkiadakis,[51] A. Hamilton,[20] B.-Y. Han,[48] J. Y. Han,[48] R. Handler,[58] F. Happacher,[19] K. Hara,[54] D. Hare,[51] M. Hare,[55] S. Harper,[41] R. F. Harr,[57] R. M. Harris,[17] M. Hartz,[46] K. Hatakeyama,[49] J. Hauser,[8] C. Hays,[41] M. Heck,[26] A. Heijboer,[44] B. Heinemann,[28] J. Heinrich,[44] C. Henderson,[32] M. Herndon,[58] J. Heuser,[26] S. Hewamanage,[4] D. Hidas,[16] C. S. Hill,[10,c] D. Hirschbuehl,[26] A. Hocker,[17] S. Hou,[1] M. Houlden,[29] S.-C. Hsu,[9] B. T. Huffman,[41] R. E. Hughes,[38] U. Husemann,[59] J. Huston,[35] J. Incandela,[10] G. Introzzi,[45] M. Iori,[50] A. Ivanov,[7] B. Iyutin,[32] E. James,[17] B. Jayatilaka,[16] D. Jeans,[50] E. J. Jeon,[27] S. Jindariani,[18] W. Johnson,[7] M. Jones,[47] K. K. Joo,[27] S. Y. Jun,[12] J. E. Jung,[27] T. R. Junk,[24] T. Kamon,[52] D. Kar,[18] P. E. Karchin,[57] Y. Kato,[40] R. Kephart,[17] U. Kerzel,[26] V. Khotilovich,[52] B. Kilminster,[38] D. H. Kim,[27] H. S. Kim,[27] J. E. Kim,[27] M. J. Kim,[17] S. B. Kim,[27] S. H. Kim,[54] Y. K. Kim,[13] N. Kimura,[54] L. Kirsch,[6] S. Klimenko,[18] M. Klute,[32] B. Knuteson,[32] B. R. Ko,[16] S. A. Koay,[10] K. Kondo,[56] D. J. Kong,[27] J. Konigsberg,[18] A. Korytov,[18] A. V. Kotwal,[16] J. Kraus,[24] M. Kreps,[26] J. Kroll,[44] N. Krumnack,[4] M. Kruse,[16] V. Krutelyov,[10] T. Kubo,[54] S. E. Kuhlmann,[2] T. Kuhr,[26] N. P. Kulkarni,[57] Y. Kusakabe,[56] S. Kwang,[13] A. T. Laasanen,[47] S. Lai,[33] S. Lami,[45] S. Lammel,[17] M. Lancaster,[30] R. L. Lander,[7] K. Lannon,[38] A. Lath,[51] G. Latino,[45] I. Lazzizzera,[42] T. LeCompte,[2] J. Lee,[48] J. Lee,[27] Y. J. Lee,[27] S. W. Lee,[52,q] R. Lefèvre,[20] N. Leonardo,[32] S. Leone,[45] S. Levy,[13] J. D. Lewis,[17] C. Lin,[59] C. S. Lin,[28] J. Linacre,[41] M. Lindgren,[17] E. Lipeles,[9] A. Lister,[7] D. O. Litvintsev,[17] T. Liu,[17] N. S. Lockyer,[44] A. Loginov,[59] M. Loreti,[42] L. Lovas,[14] R.-S. Lu,[1] D. Lucchesi,[42] J. Lueck,[26] C. Luci,[50] P. Lujan,[28] P. Lukens,[17] G. Lungu,[18] L. Lyons,[41] J. Lys,[28] R. Lysak,[14] E. Lytken,[47] P. Mack,[26] D. MacQueen,[33] R. Madrak,[17] K. Maeshima,[17] K. Makhoul,[32] T. Maki,[23] P. Maksimovic,[25] S. Malde,[41] S. Malik,[30] G. Manca,[29] A. Manousakis,[15,a] F. Margaroli,[47] C. Marino,[26] C. P. Marino,[24] A. Martin,[59] M. Martin,[25] V. Martin,[21,j] M. Martínez,[3] R. Martínez-Ballarín,[31] T. Maruyama,[54] P. Mastrandrea,[50] T. Masubuchi,[54] M. E. Mattson,[57] P. Mazzanti,[5] K. S. McFarland,[48] P. McIntyre,[52] R. McNulty,[29,i] A. Mehta,[29] P. Mehtala,[23] S. Menzemer,[11,k] A. Menzione,[45] P. Merkel,[47] C. Mesropian,[49] A. Messina,[35] T. Miao,[17] N. Miladinovic,[6] J. Miles,[32] R. Miller,[35] C. Mills,[22] M. Milnik,[26] A. Mitra,[1] G. Mitselmakher,[18] H. Miyake,[54] S. Moed,[22] N. Moggi,[5] C. S. Moon,[27] R. Moore,[17] M. Morello,[45] P. Movilla Fernandez,[28] J. Mülmenstädt,[28] A. Mukherjee,[17] Th. Muller,[26] R. Mumford,[25] P. Murat,[17] M. Mussini,[5] J. Nachtman,[17] Y. Nagai,[54]

A. Nagano,[54] J. Naganoma,[56] K. Nakamura,[54] I. Nakano,[39] A. Napier,[55] V. Necula,[16] C. Neu,[44] M. S. Neubauer,[24] J. Nielsen,[28,f] L. Nodulman,[2] M. Norman,[9] O. Norniella,[24] E. Nurse,[30] S. H. Oh,[16] Y. D. Oh,[27] I. Oksuzian,[18] T. Okusawa,[40] R. Oldeman,[29] R. Orava,[23] K. Osterberg,[23] S. Pagan Griso,[42] C. Pagliarone,[45] E. Palencia,[17] V. Papadimitriou,[17] A. Papaikonomou,[26] A. A. Paramonov,[13] B. Parks,[38] S. Pashapour,[33] J. Patrick,[17] G. Pauletta,[53] M. Paulini,[12] C. Paus,[32] D. E. Pellett,[7] A. Penzo,[53] T. J. Phillips,[16] G. Piacentino,[45] J. Piedra,[43] L. Pinera,[18] K. Pitts,[24] C. Plager,[8] L. Pondrom,[58] X. Portell,[3] O. Poukhov,[15] N. Pounder,[41] F. Prakoshyn,[15] A. Pronko,[17] J. Proudfoot,[2] F. Ptohos,[17,h] G. Punzi,[45] J. Pursley,[58] J. Rademacker,[41,c] A. Rahaman,[46] V. Ramakrishnan,[58] N. Ranjan,[47] I. Redondo,[31] B. Reisert,[17] V. Rekovic,[36] P. Renton,[41] M. Rescigno,[50] S. Richter,[26] F. Rimondi,[5] L. Ristori,[45] A. Robson,[21] T. Rodrigo,[11] E. Rogers,[24] S. Rolli,[55] R. Roser,[17] M. Rossi,[53] R. Rossin,[10] P. Roy,[33] A. Ruiz,[11] J. Russ,[12] V. Rusu,[17] H. Saarikko,[23] A. Safonov,[52] W. K. Sakumoto,[48] G. Salamanna,[50] O. Saltó,[3] L. Santi,[53] S. Sarkar,[50] L. Sartori,[45] K. Sato,[17] A. Savoy-Navarro,[43] T. Scheidle,[26] P. Schlabach,[17] E. E. Schmidt,[17] M. A. Schmidt,[13] M. P. Schmidt,[59] M. Schmitt,[37] T. Schwarz,[7] L. Scodellaro,[11] A. L. Scott,[10] A. Scribano,[45] F. Scuri,[45] A. Sedov,[47] S. Seidel,[36] Y. Seiya,[40] A. Semenov,[15] L. Sexton-Kennedy,[17] A. Sfyria,[20] S. Z. Shalhout,[57] M. D. Shapiro,[28] T. Shears,[29] P. F. Shepard,[46] D. Sherman,[22] M. Shimojima,[54,n] M. Shochet,[13] Y. Shon,[58] I. Shreyber,[20] A. Sidoti,[45] P. Sinervo,[33] A. Sisakyan,[15] A. J. Slaughter,[17] J. Slaunwhite,[38] K. Sliwa,[55] J. R. Smith,[7] F. D. Snider,[17] R. Snihur,[33] M. Soderberg,[34] A. Soha,[7] S. Somalwar,[51] V. Sorin,[35] J. Spalding,[17] F. Spinella,[45] T. Spreitzer,[33] P. Squillacioti,[45] M. Stanitzki,[59] R. St. Denis,[21] B. Stelzer,[8] O. Stelzer-Chilton,[41] D. Stentz,[37] J. Strologas,[36] D. Stuart,[10] J. S. Suh,[27] A. Sukhanov,[18] H. Sun,[55] I. Suslov,[15] T. Suzuki,[54] A. Taffard,[24,e] R. Takashima,[39] Y. Takeuchi,[54] R. Tanaka,[39] M. Tecchio,[34] P. K. Teng,[1] K. Terashi,[49] J. Thom,[17,g] A. S. Thompson,[21] G. A. Thompson,[24] E. Thomson,[44] P. Tipton,[59] V. Tiwari,[12] S. Tkaczyk,[17] D. Toback,[52] S. Tokar,[14] K. Tollefson,[35] T. Tomura,[54] D. Tonelli,[17] S. Torre,[19] D. Torretta,[17] S. Tourneur,[43] W. Trischuk,[33] Y. Tu,[44] N. Turini,[45] F. Ukegawa,[54] S. Uozumi,[54] S. Vallecorsa,[20] N. van Remortel,[23] A. Varganov,[34] E. Vataga,[36] F. Vázquez,[18,l] G. Velev,[17] C. Vellidis,[45,a] V. Veszpremi,[47] M. Vidal,[31] R. Vidal,[17] I. Vila,[11] R. Vilar,[11] T. Vine,[30] M. Vogel,[36] I. Volobouev,[28,q] G. Volpi,[45] F. Würthwein,[9] P. Wagner,[44] R. G. Wagner,[2] R. L. Wagner,[17] J. Wagner-Kuhr,[26] W. Wagner,[26] T. Wakisaka,[40] R. Wallny,[8] S. M. Wang,[1] A. Warburton,[33] D. Waters,[30] M. Weinberger,[52] W. C. Wester III,[17] B. Whitehouse,[55] D. Whiteson,[44,e] A. B. Wicklund,[2] E. Wicklund,[17] G. Williams,[33] H. H. Williams,[44] P. Wilson,[17] B. L. Winer,[38] P. Wittich,[17,g] S. Wolbers,[17] C. Wolfe,[13] T. Wright,[34] X. Wu,[20] S. M. Wynne,[29] A. Yagil,[9] K. Yamamoto,[40] J. Yamaoka,[51] T. Yamashita,[39] C. Yang,[59] U. K. Yang,[13,m] Y. C. Yang,[27] W. M. Yao,[28] G. P. Yeh,[17] J. Yoh,[17] K. Yorita,[13] T. Yoshida,[40] G. B. Yu,[48] I. Yu,[27] S. S. Yu,[17] J. C. Yun,[17] L. Zanello,[50] A. Zanetti,[53] I. Zaw,[22] X. Zhang,[24] Y. Zheng,[8,b] and S. Zucchelli[5]

(CDF Collaboration)

[1]*Institute of Physics, Academia Sinica, Taipei, Taiwan 11529, Republic of China*
[2]*Argonne National Laboratory, Argonne, Illinois 60439, USA*
[3]*Institut de Fisica d'Altes Energies, Universitat Autonoma de Barcelona, E-08193, Bellaterra (Barcelona), Spain*
[4]*Baylor University, Waco, Texas 76798, USA*
[5]*Istituto Nazionale di Fisica Nucleare, University of Bologna, I-40127 Bologna, Italy*
[6]*Brandeis University, Waltham, Massachusetts 02254, USA*
[7]*University of California, Davis, Davis, California 95616, USA*
[8]*University of California, Los Angeles, Los Angeles, California 90024, USA*
[9]*University of California, San Diego, La Jolla, California 92093, USA*
[10]*University of California, Santa Barbara, Santa Barbara, California 93106, USA*
[11]*Instituto de Fisica de Cantabria, CSIC-University of Cantabria, 39005 Santander, Spain*
[12]*Carnegie Mellon University, Pittsburgh, Pennsylvania 15213, USA*
[13]*Enrico Fermi Institute, University of Chicago, Chicago, Illinois 60637, USA*
[14]*Comenius University, 842 48 Bratislava, Slovakia; Institute of Experimental Physics, 040 01 Kosice, Slovakia*
[15]*Joint Institute for Nuclear Research, RU-141980 Dubna, Russia*
[16]*Duke University, Durham, North Carolina 27708, USA*
[17]*Fermi National Accelerator Laboratory, Batavia, Illinois 60510, USA*
[18]*University of Florida, Gainesville, Florida 32611, USA*
[19]*Laboratori Nazionali di Frascati, Istituto Nazionale di Fisica Nucleare, I-00044 Frascati, Italy*
[20]*University of Geneva, CH-1211 Geneva 4, Switzerland*
[21]*Glasgow University, Glasgow G12 8QQ, United Kingdom*
[22]*Harvard University, Cambridge, Massachusetts 02138, USA*
[23]*Division of High Energy Physics, Department of Physics, University of Helsinki and Helsinki Institute of Physics, FIN-00014, Helsinki, Finland*

[24]University of Illinois, Urbana, Illinois 61801, USA
[25]The Johns Hopkins University, Baltimore, Maryland 21218, USA
[26]Institut für Experimentelle Kernphysik, Universität Karlsruhe, 76128 Karlsruhe, Germany
[27]Center for High Energy Physics: Kyungpook National University, Daegu 702-701, Korea; Seoul National University, Seoul 151-742, Korea; Sungkyunkwan University, Suwon 440-746, Korea; Korea Institute of Science and Technology Information, Daejeon, 305-806, Korea; Chonnam National University, Gwangju, 500-757, Korea
[28]Ernest Orlando Lawrence Berkeley National Laboratory, Berkeley, California 94720, USA
[29]University of Liverpool, Liverpool L69 7ZE, United Kingdom
[30]University College London, London WC1E 6BT, United Kingdom
[31]Centro de Investigaciones Energeticas Medioambientales y Tecnologicas, E-28040 Madrid, Spain
[32]Massachusetts Institute of Technology, Cambridge, Massachusetts 02139, USA
[33]Institute of Particle Physics: McGill University, Montréal, Canada H3A 2T8 and University of Toronto, Toronto, Canada M5S 1A7
[34]University of Michigan, Ann Arbor, Michigan 48109, USA
[35]Michigan State University, East Lansing, Michigan 48824, USA
[36]University of New Mexico, Albuquerque, New Mexico 87131, USA
[37]Northwestern University, Evanston, Illinois 60208, USA
[38]The Ohio State University, Columbus, Ohio 43210, USA
[39]Okayama University, Okayama 700-8530, Japan
[40]Osaka City University, Osaka 588, Japan
[41]University of Oxford, Oxford OX1 3RH, United Kingdom
[42]Istituto Nazionale di Fisica Nucleare, University of Padova, Sezione di Padova-Trento, I-35131 Padova, Italy
[43]LPNHE, Universite Pierre et Marie Curie/IN2P3-CNRS, UMR7585, Paris, F-75252 France
[44]University of Pennsylvania, Philadelphia, Pennsylvania 19104, USA
[45]Istituto Nazionale di Fisica Nucleare Pisa, Universities of Pisa, Siena, and Scuola Normale Superiore, I-56127 Pisa, Italy
[46]University of Pittsburgh, Pittsburgh, Pennsylvania 15260, USA
[47]Purdue University, West Lafayette, Indiana 47907, USA
[48]University of Rochester, Rochester, New York 14627, USA
[49]The Rockefeller University, New York, New York 10021, USA
[50]Istituto Nazionale di Fisica Nucleare, Sezione di Roma 1, University of Rome "La Sapienza," I-00185 Roma, Italy
[51]Rutgers University, Piscataway, New Jersey 08855, USA
[52]Texas A&M University, College Station, Texas 77843, USA
[53]Istituto Nazionale di Fisica Nucleare, University of Trieste/Udine, Italy
[54]University of Tsukuba, Tsukuba, Ibaraki 305, Japan
[55]Tufts University, Medford, Massachusetts 02155, USA
[56]Waseda University, Tokyo 169, Japan
[57]Wayne State University, Detroit, Michigan 48201, USA
[58]University of Wisconsin, Madison, Wisconsin 53706, USA
[59]Yale University, New Haven, Connecticut 06520, USA

(Received 22 October 2007; published 19 February 2008)

A direct measurement of the total decay width of the W boson Γ_W is presented using 350 pb^{-1} of data from $p\bar{p}$ collisions at $\sqrt{s} = 1.96$ TeV collected with the CDF II detector at the Fermilab Tevatron. The width is determined by normalizing predicted signal and background distributions to 230 185 W candidates decaying to $e\nu$ and $\mu\nu$ in the transverse-mass region $50 < M_T < 90$ GeV and then fitting the predicted shape to 6055 events in the high-M_T region, $90 < M_T < 200$ GeV. The result is $\Gamma_W = 2032 \pm 45_{\text{stat}} \pm 57_{\text{syst}}$ MeV, consistent with the standard model expectation.

DOI: 10.1103/PhysRevLett.100.071801 PACS numbers: 13.38.Be, 14.70.Fm

The decay widths of the W and Z bosons that mediate the weak interaction are precisely predicted within the standard model (SM). At Born level the W width Γ_W and mass M_W are related through the precisely determined Fermi coupling constant, G_F. Beyond leading order, higher-order electroweak (EW) and quantum-chromodynamic (QCD) corrections, $\delta_{\text{EW}} \approx -0.4\%$ and $\delta_{\text{QCD}} \approx 2.5\%$, respectively, modify the relation such that $\Gamma_W = \frac{3G_F M_W^3}{\sqrt{8}\pi}(1 + \delta_{\text{EW}} + \delta_{\text{QCD}})$ [1,2]. The uncertainty on the SM prediction $\Gamma_W = 2091 \pm 2$ MeV is dominated by the uncertainty on M_W with smaller contributions from the uncertainties on the higher-order corrections [3]. Uncertainties on SM parameters, such as the Higgs boson mass, affect this prediction very weakly, and so a measurement allows an unambiguous test of the SM that can also be used to constrain other SM parameters such as the V_{cs}

Cabibbo-Kobayashi-Maskawa matrix element [4]. The combination of published direct measurements of Γ_W from $p\bar{p}$ collisions at the Tevatron [5] and e^+e^- collisions at LEP-II [6] has an uncertainty of 2.7% with the most precise determination from a single experiment (ALEPH) having an uncertainty of 5.1%. The most precise indirect determination [7] of Γ_W from a measurement of the ratio $R = \frac{\sigma(p\bar{p}\to W\to \ell\nu)}{\sigma(p\bar{p}\to Z\to \ell^+\ell^-)}$ has an uncertainty of 2%.

This Letter presents the world's most precise direct determination of Γ_W from a single experiment. The analysis uses $W\to e\nu(\mu\nu)$ data with integrated luminosities of 370(330) pb^{-1} collected by the CDF II detector at the Fermilab Tevatron.

Neutrinos are undetectable by the CDF II detector and hence the invariant mass of the W boson cannot be reconstructed. Γ_W is therefore determined from a fit to the distribution of the W transverse mass $M_T = \sqrt{2(p_T^\ell p_T^\nu - \vec{p}_T^\ell \cdot \vec{p}_T^\nu)}$, where $\vec{p}_T^\ell$ and $\vec{p}_T^\nu$ are the measured transverse momentum of the charged lepton and the transverse momentum of the neutrino as inferred from the observed missing transverse energy, respectively.

The components of the CDF II detector relevant to this analysis are described briefly here; a more complete description can be found elsewhere [8]. A silicon microstrip detector [9] is used to measure the distance of closest approach in the transverse plane, d_0, of charged particles to the beam line. The momenta of charged particles are measured using a 96-layer drift chamber (COT) [10] inside a 1.4 T solenoid. Electromagnetic and hadronic calorimeters, arranged in a projective tower geometry, cover the pseudorapidity range $|\eta| < 3.64$ [11]. In the region $|\eta| < 1.0$, a lead/scintillator electromagnetic calorimeter (CEM) [12] measures electron energies and proportional chambers embedded at the shower maximum provide further information on shower shapes and positions. A system of drift chambers outside the calorimeters is used to identify muons in the region $|\eta| < 1.0$ [13].

$W\to e\nu$ candidate events are selected by a large transverse energy electron trigger, and the electron shower is required to have transverse energy $E_T^e > 25$ GeV [11] in the CEM. The ratio of the energy measured in the CEM and the charged-track momentum measured in the COT, E/p, must satisfy $0.8 < E/p < 1.3$. The ratio of energy deposited in the hadronic (HAD) and CEM calorimeter towers is required to satisfy $E_{\text{HAD}}/E_{\text{CEM}} < 0.07$. The electron shower must be contained within a fiducial region of the CEM, away from calorimeter cell boundaries, and have a typical electron lateral shower profile. Contamination by $Z\to e^+e^-$ events is reduced by rejecting events with an additional high p_T track of opposite charge pointing to an uninstrumented region of the calorimeter.

$W\to \mu\nu$ candidate events are selected by a large p_T muon trigger and are required to contain a COT track, well matched to a track segment in the muon chambers, with $p_T^\mu > 25$ GeV. The energy deposited in the CEM and HAD must be consistent with the passage of a minimum-ionizing particle. Requirements on the track d_0 and fit χ^2 are imposed to reject background. Events consistent with cosmic rays or those with an additional high-p_T track consistent with $Z\to \mu^+\mu^-$ decays are removed.

The existence of a neutrino is inferred from a transverse momentum imbalance. The missing transverse momentum, $\vec{p}_T^\nu \equiv -(\vec{p}_T^\ell + \vec{u})$, must satisfy $p_T^\nu > 25$ GeV. The components of the recoil transverse energy vector $\vec{u}$ are defined as $\sum_i E_i \sin\theta_i(\cos\phi_i, \sin\phi_i)$, for calorimeter towers i with $|\eta| < 3.64$, excluding those traversed by and surrounding the charged lepton. $\vec{u}$ receives contributions from initial-state QCD radiation, underlying-event energy, final-state photon radiation, and overlapping $p\bar{p}$ interactions. To reduce backgrounds and improve transverse-mass resolution, the recoil energy must satisfy $u < 20$ GeV. The $W\to e\nu(\mu\nu)$ sample consists of 127 432 (108 808) candidate events in the range $50 < M_T < 200$ GeV and 3436 (2619) in the high M_T range of $90 < M_T < 200$ GeV.

Since the W and Z bosons share a common production mechanism and the momenta of Z bosons can be directly reconstructed from their decay products, $Z\to \ell^+\ell^-$ decays are used to model the detector's response to $W\to \ell\nu$ events. Samples of $Z\to e^+e^-(\mu^+\mu^-)$ candidates are selected by requiring two charged leptons, with the same requirements as the W lepton candidates, with the exception that the muon chamber track match requirement is removed for one of the muons in the $Z\to \mu^+\mu^-$ pair. The $\ell^+\ell^-$ invariant mass is required to satisfy $80 < M^{\ell\ell} < 100$ GeV. 2909 (6721) $Z\to e^+e^-(\mu^+\mu^-)$ events with recoil energy $u < 20$ GeV are used to determine the scale and resolution of the lepton energy and momentum measurements. A second set of $Z\to e^+e^-(\mu^+\mu^-)$ events with the u cut replaced by a di-lepton transverse momentum cut, $p_T^{\ell\ell} < 50$ GeV, are used to constrain the W boson's transverse momentum spectrum and to provide an empirical model of the recoil.

The W boson M_T spectrum is modeled using a Monte Carlo (MC) simulation. The CTEQ6M [14] parton distribution functions (PDFs) are used, and W boson invariant masses $\sqrt{\hat{s}}$ are generated according to an energy-dependent Breit-Wigner distribution: $\sigma(\hat{s}) \sim [\hat{s}(1 - M_W^2/\hat{s})^2 + \hat{s}\Gamma_W^2/M_W^2]^{-1}$. Higher-order QCD effects are included by generating the W bosons with a p_T distribution from a resummed next-to-leading order (NLO) QCD calculation [15] with the nonperturbative prescription of [16]. Photon radiation from the charged lepton is simulated using a $\mathcal{O}(\alpha)$ matrix-element calculation [17]. Corrections for EW box diagrams are applied from [18].

The charged leptons and radiated photons are passed through a custom detector simulation that models in detail the energy loss due to ionization and bremsstrahlung. The simulation also includes a parametric model of the $\vec{u}$

measurement as a function of the boson p_T, tuned on data as described below. The same kinematic and geometric cuts used to select candidate events in the data are applied to the simulation.

This measurement relies on the accurate modeling of the M_T distribution over a wide range. The most important sources of systematic uncertainty affecting the M_T shape arise from the charged-lepton energy and momentum scales and resolutions, the recoil modeling, and the presence of backgrounds. All systematic uncertainties are evaluated by varying parameters in the simulation and then fitting the resulting M_T spectra with the nominal spectra. Uncertainties have been calculated separately for the fit region $M_T^{\rm cut} < M_T < 200$ GeV for $M_T^{\rm cut}$ values ranging from 80 to 110 GeV. While the statistical uncertainty decreases as $M_T^{\rm cut}$ is lowered, the systematic uncertainty increases. A value of $M_T^{\rm cut} = 90$ GeV gives the smallest total uncertainty. Backgrounds are added to the simulation M_T spectra which are then normalized to the number of data events in the region $50 < M_T < 90$ GeV.

The COT momentum scale is determined from a fit to the $Z \to \mu^+\mu^-$ invariant-mass distribution with the Z mass M_Z constrained to the world average value [3]. A consistent COT momentum scale is obtained from fits to the $\mu^+\mu^-$ invariant-mass distributions from J/ψ and Υ decays [8]. The difference between the three determinations has a negligible effect on this analysis. The contribution to the uncertainty on Γ_W in the $W \to \mu\nu$ channel $\Delta\Gamma_W^{\mu\nu}$ arising from the 0.04% uncertainty in the COT momentum scale, due to the $Z \to \mu^+\mu^-$ statistics, is $\Delta\Gamma_W^{\mu\nu} = 17$ MeV.

By scaling the resolutions predicted by a GEANT [19] simulation of the COT to match the observed di-muon invariant-mass distribution in $Z \to \mu^+\mu^-$ decays, a momentum resolution of $\sigma(1/p_T) = (5.4 \pm 0.2) \times 10^{-4}$ GeV^{-1} is obtained. A consistent $\sigma(1/p_T)$ is determined using the E/p distribution of the $W \to e\nu$ data. The combined uncertainties from the $Z \to \mu^+\mu^-$ and E/p fits for the COT resolution give $\Delta\Gamma_W^{\mu\nu} = 26$ MeV.

The CEM energy scale and resolution are determined from fits to the $Z \to e^+e^-$ invariant-mass distribution with M_Z constrained to the world average value [3] and to the E/p distribution of electrons in $W \to e\nu$ events. The scales determined from the two methods are consistent and are combined with an uncertainty of 0.04%. The contribution to the uncertainty on Γ_W in the $W \to e\nu$ channel $\Delta\Gamma_W^{e\nu}$ arising from this uncertainty is $\Delta\Gamma_W^{e\nu} = 17$ MeV.

Determinations of the CEM resolution term κ defined by the CEM resolution function $\sigma(E)/E = 13.5\%/\sqrt{E_T(\text{GeV})} \oplus \kappa$ [12] from E/p and $Z \to e^+e^-$ fits differ by 1.6σ. They are combined and an uncertainty is assigned that spans both values, as well as the values obtained when the E/p fit region is varied, to give $\kappa = 1.1 \pm 0.4\%$. This uncertainty on the CEM resolution gives $\Delta\Gamma_W^{e\nu} = 31$ MeV.

Energy loss by electrons and photons in the solenoid coil and associated material prior to the CEM, as well as energy leakage into the hadronic calorimeter, are parametrized based on the results of a GEANT simulation. In addition to these simulated sources of CEM nonlinearity, an additional per-particle intrinsic nonlinearity is determined from the $W(Z) \to e\nu(e^+e^-)$ data by fitting the E/p distribution in bins of E_T. Its uncertainty gives $\Delta\Gamma_W^{e\nu} = 12$ MeV, resulting in a total uncertainty of 21 MeV on $\Gamma_W^{e\nu}$ from the uncertainties on the electron energy scale determination. Finally, uncertainties in the modeling of very low-energy photons and the amount of passive material prior to the COT give $\Delta\Gamma_W^{e\nu} = 13$ MeV.

The recoil transverse energy vector $\vec{u}$ is used to determine $\vec{p}_T^{\,\nu}$ and hence M_T. Since $\vec{u}$ comes predominantly from initial-state QCD radiation, which is balanced by the W or Z p_T, we form an empirical model of $\vec{u}$ as a function of $p_T^{\ell\ell}$. The parameters of the model are varied according to the covariance matrices obtained in fits to Z data. The resulting uncertainties on $\vec{u}$ from the recoil model give $\Delta\Gamma_W^{e\nu}(\Delta\Gamma_W^{\mu\nu}) = 54(49)$ MeV. The uncertainty in the modeling of the p_T^W distribution is determined by fitting the $p_T^{\ell\ell}$ distribution in $Z \to \ell^+\ell^-$ decays and results in a 7 MeV common uncertainty on Γ_W.

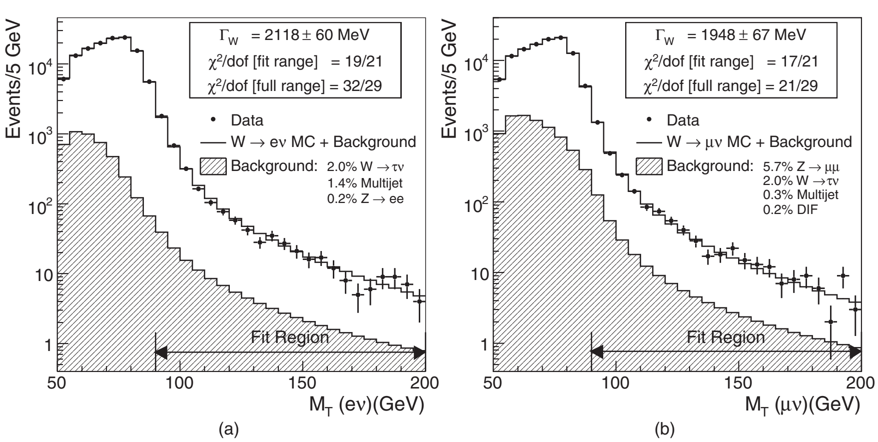

FIG. 1. The transverse-mass distributions of the $W \to e\nu$ data (a) and $W \to \mu\nu$ data (b) compared to the best fit.

Several background processes can mimic the W signal. The process $W \rightarrow \tau\nu \rightarrow \ell\nu\nu\nu$ has a signature similar to $W \rightarrow \ell\nu$ decays, but with lower M_T. $Z \rightarrow \ell^+\ell^-$ events, where only one lepton is identified, can be reconstructed as W candidates. These two backgrounds can be accurately determined from MC simulation. QCD multijet backgrounds arise when one jet mimics a charged lepton and another is mismeasured to produce an energy imbalance. Since the region with apparently low p_T^ν is enriched in QCD background, the background is estimated from a fit to the p_T^ν distribution in events where the p_T^ν and low M_T cut are not applied and in which some of the charged-lepton identification cuts have been reversed. The signal spectrum is taken from the simulation. A decay-in-flight (DIF) background to the $W \rightarrow \mu\nu$ signal arises when kaons or pions decay to $\mu\nu$ inside the COT, resulting in mismeasured p_T^μ and a large χ^2 value between the COT hits assigned to the track and the fitted track trajectory. This background is estimated from the χ^2 and d_0 distributions of $W \rightarrow \mu\nu$ events using $Z \rightarrow \mu^+\mu^-$ events as a reference sample with negligible background. The background fractions over the entire region $50 < M_T < 200$ GeV are indicated in Fig. 1. In the $90 < M_T < 200$ GeV fit region the background fraction is $4.0 \pm 0.2\%$ ($10.8 \pm 0.3\%$) in the $e\nu(\mu\nu)$ channel. Varying the backgrounds within these overall normalization uncertainties, as well as varying their M_T shapes, gives $\Delta\Gamma_W^{e\nu}(\Delta\Gamma_W^{\mu\nu}) = 32(33)$ MeV.

We also investigate small systematic uncertainties due to PDFs, M_W, EW corrections, lepton identification, and acceptance. The uncertainty on Γ_W arising from PDFs is determined using the variations defined by the CTEQ6M PDF eigenvector basis [14] which span a 90% confidence interval. The resulting Γ_W shifts are divided by 1.6 to obtain 1σ uncertainties [20], giving $\Delta\Gamma_W = 16$ MeV in both channels. A systematic uncertainty of 12 MeV is added in quadrature to this to account for higher-order QCD effects not implemented in the MC simulation. These were estimated from a comparison of the width obtained using NLO and next-to-next-to-leading order (NNLO) PDFs [21]. Varying M_W by the uncertainty of ± 29 MeV [3] from the central value of 80.403 GeV changes Γ_W by ∓ 9 MeV in each channel.

The impact of higher-order EW corrections is determined by comparing simulated samples of $W \rightarrow \ell\nu\gamma$ and $W \rightarrow \ell\nu\gamma\gamma$ events generated by PHOTOS [22]. Uncertainties on $\Gamma_W^{e\nu}(\Gamma_W^{\mu\nu})$ of 8(1) MeV were obtained. The correction due to EW box diagrams was determined to be 12 MeV in both channels. A systematic uncertainty of 6 MeV in this correction was assigned from its dependence on the recoil resolution.

The uncertainty in simulating lepton identification variables was constrained from $Z \rightarrow \ell^+\ell^-$ decays and gives $\Delta\Gamma_W^{e\nu}(\Delta\Gamma_W^{\mu\nu}) = 10(6)$ MeV. Variations in the simulation of the detector acceptance results in further small uncertainties of 3(4) MeV in the $e\nu(\mu\nu)$ channel. Table I summarizes the sources of uncertainty described above.

TABLE I. The sources of uncertainty (in MeV) on Γ_W for the $W \rightarrow e\nu$ and $W \rightarrow \mu\nu$ measurements. If there is a correlated source of error between the two measurements its contribution to each measurement is listed in the third column, labeled C.

Source	$\Delta\Gamma_W^{e\nu}$	$\Delta\Gamma_W^{\mu\nu}$	C
Statistics	60	67	
Lepton E or p scale	21	17	12
Lepton E or p resolution	31	26	
Electron energy loss simulation	13		
Recoil model	54	49	
p_T^W	7	7	7
Backgrounds	32	33	
PDFs	20	20	20
M_W	9	9	9
EW radiative corrections	10	6	6
Lepton ID/acceptance	10	7	
Total systematic	79	71	27
Total (statistic + systematic)	99	98	27

A binned likelihood fit to simulated M_T spectra with Γ_W as a free parameter over the region $90 < M_T < 200$ GeV gives $\Gamma_W^{e\nu} = 2118 \pm 60_{\rm stat}$ MeV and $\Gamma_W^{\mu\nu} = 1948 \pm 67_{\rm stat}$ MeV. Figure 1 shows the M_T distributions of the data with the best fits. The two results have a common uncertainty of 27 MeV and are combined using the BLUE method [23] to give $\Gamma_W = 2032 \pm 45_{\rm stat} \pm 57_{\rm syst}$ MeV. The combination has a χ^2 of 1.6 and a total uncertainty of 73 MeV. No statistically significant difference is found between fits using positively or negatively charged leptons. As a cross-check, Γ_W was also determined from a fit to p_T^ℓ, which has a different sensitivity to many of the systematics, and a value of Γ_W consistent with the M_T fit at the $<1\sigma$ level was obtained.

The result presented in this Letter is the most precise direct measurement of the W width. It can be combined with published Tevatron direct width measurements [5] to give a Tevatron average of $\Gamma_W = 2056 \pm 62$ MeV. A further combination with the preliminary value obtained from e^+e^- collisions, $\Gamma_W = 2196 \pm 84$ MeV [24], gives a new world average value of $\Gamma_W = 2106 \pm 50$ MeV, in good agreement with the SM prediction.

We thank the Fermilab staff and the technical staffs of the participating institutions for their vital contributions. This work was supported by the US Department of Energy and National Science Foundation; the Italian Istituto Nazionale di Fisica Nucleare; the Ministry of Education, Culture, Sports, Science, and Technology of Japan; the Natural Sciences and Engineering Research Council of Canada; the National Science Council of the Republic of China; the Swiss National Science Foundation; the A. P. Sloan Foundation; the Bundesministerium für Bildung und Forschung, Germany; the Korean Science and Engineering Foundation and the Korean Research Foundation; the Science and Technology Facilities Council and the Royal

Society, UK; the Institut National de Physique Nucleaire et Physique des Particules/CNRS; the Russian Foundation for Basic Research; the Comisión Interministerial de Ciencia y Tecnología, Spain; the European Community's Human Potential Programme; the Slovak R&D Agency; and the Academy of Finland.

[a]Visiting scientist from University of Athens, 15784 Athens, Greece.
[b]Visiting scientist from Chinese Academy of Sciences, Beijing 100864, China.
[c]Visiting scientist from University of Bristol, Bristol, United Kingdom.
[d]Visiting scientist from University Libre de Bruxelles, B-1050 Brussels, Belgium.
[e]Visiting scientist from University of California, Irvine, Irvine, CA 92697, USA.
[f]Visiting scientist from University of California, Santa Cruz, Santa Cruz, CA 95064, USA.
[g]Visiting scientist from Cornell University, Ithaca, NY 14853, USA.
[h]Visiting scientist from University of Cyprus, Nicosia CY-1678, Cyprus.
[i]Visiting scientist from University College Dublin, Dublin 4, Ireland.
[j]Visiting scientist from University of Edinburgh, Edinburgh, United Kingdom.
[k]Visiting scientist from University of Heidelberg, D-69120 Heidelberg, Germany.
[l]Visiting scientist from Universidad Iberoamericana, Mexico D.F., Mexico.
[m]Visiting scientist from University of Manchester, Manchester, United Kingdom.
[n]Visiting scientist from Nagasaki Institute of Applied Science, Nagasaki, Japan.
[o]Visiting scientist from University de Oviedo, E-33007 Oviedo, Spain.
[p]Visiting scientist from Queen Mary, University of London, London, United Kingdom.
[q]Visiting scientist from Texas Tech University, Lubbock, TX 79409, USA.
[r]Visiting scientist from IFIC (CSIC-Universitat de Valencia), 46071 Valencia, Spain.

[1] J. L. Rosner, M. P. Worah, and T. Takeuchi, Phys. Rev. D **49**, 1363 (1994).
[2] Throughout this Letter units of $\hbar = c = 1$ are used such that momenta and masses are in units of MeV or GeV.
[3] W.-M. Yao *et al.*, J. Phys. G **33**, 1 (2006).
[4] P. B. Renton, Rep. Prog. Phys. **65**, 1271 (2002).
[5] V. Abazov *et al.*, (CDF and D0 Collaborations), Phys. Rev. D **70**, 092008 (2004).
[6] S. Schael *et al.* (ALEPH Collaboration), Eur. Phys. J. C **47**, 309 (2006); G. Abbiendi *et al.* (OPAL Collaboration), *ibid.* **45**, 307 (2006); P. Achard *et al.* (L3 Collaboration), *ibid.* **45**, 569 (2006); P. Abreu *et al.* (DELPHI Collaboration), Phys. Lett. B **511**, 159 (2001).
[7] D. Acosta *et al.* (CDF Collaboration), Phys. Rev. Lett. **94**, 091803 (2005).
[8] T. Aaltonen *et al.* (CDF Collaboration), arXiv:0708.3642.
[9] A. Sill *et al.*, Nucl. Instrum. Methods Phys. Res., Sect. A **447**, 1 (2000); A. Affolder *et al.*, *ibid.* **453**, 84 (2000).
[10] A. Affolder *et al.*, Nucl. Instrum. Methods Phys. Res., Sect. A **526**, 249 (2004).
[11] CDF uses a cylindrical coordinate system in which ϕ is the azimuthal angle, θ is the polar angle, and z points in the proton beam direction. The pseudorapidity, η, is defined as $\eta \equiv -\ln\tan(\theta/2)$. The transverse plane is the plane perpendicular to the z axis. The transverse energy is defined to be $E_T = E\sin\theta$.
[12] L. Balka *et al.*, Nucl. Instrum. Methods Phys. Res., Sect. A **267**, 272 (1988).
[13] G. Ascoli *et al.*, Nucl. Instrum. Methods Phys. Res., Sect. A **268**, 33 (1988).
[14] J. Pumplin *et al.*, J. High Energy Phys. 07 (2002) 012.
[15] P. Arnold and R. Kaufman, Nucl. Phys. **B349**, 381 (1991); P. Arnold and M. Reno, *ibid.* **B319**, 37 (1989); P. Arnold, R. K. Ellis, and M. Reno, Phys. Rev. D **40**, 912 (1989).
[16] F. Landry *et al.*, Phys. Rev. D **67**, 073016 (2003).
[17] F. Berends *et al.*, Z. Phys. C **27**, 155 (1985); F. Berends and R. Kleiss, *ibid.* **27**, 365 (1985).
[18] U. Baur and D. Wackeroth, Phys. Rev. D **70**, 073015 (2004).
[19] R. Brun and F. Carminati, CERN Program Library Long Writeup No. W5013, 1993 (unpublished), version 3.15.
[20] J. Campbell, J. Huston, and W. J. Stirling, Rep. Prog. Phys. **70**, 89 (2007).
[21] A. D. Martin, R. G. Roberts, W. J. Stirling, and R. S. Thorne, Phys. Lett. B **604**, 61 (2004).
[22] E. Barberio and Z. Was, Comput. Phys. Commun. **79**, 291 (1994); E. Barberio, B. van Eijk, and Z. Was, *ibid.* **66**, 115 (1991).
[23] L. Lyons, D. Gibaut, and P. Clifford, Nucl. Instrum. Methods Phys. Res., Sect. A **270**, 110 (1988).
[24] J. Alcaraz *et al.* (LEP Electroweak Working Group), arXiv:hep-ex/0612034.